Chemistry Research Journal, 2023, 8(3):1-10
Available online www.chemrj.org

Research Article

ISSN: 2455-8990
CODEN(USA): CRJHA5

Effect of Different Pore Forming Agents on the Morphology and Porosity of Cellulose Acetate Membrane

Rehab E. Elwardany[a]*, Hassan Shokry[b,c], Ahmed A. Mustafa[a], Alaa E. Ali[a]

[a]Chemistry Department, Faculty of Science, Damanhour University, Egypt.
[b]Environmental Engineering Department, Egypt-Japan University of Science and Technology, New Borg El-Arab City, Alexandria, Egypt.
[c]Electronic Materials Researches Department, Advanced Technology and New Materials Research Institute, City of Scientific Research and Technological Applications (SRTA-City), Alexandria, Egypt
*Corresponding author. Tel: 002 01271965039. E-mail: rehabelwardany@sci.dmu.edu.eg

Abstract Cellulose acetate membrane was prepared using calcium carbonate and sodium carbonate as pore-forming agents to reach to the optimal condition for preparing CA membrane. The production of the membranes based on phase inversion techniques and FTIR was utilized to identify the surface functional groups on the prepared membrane. A scanning electron microscope (SEM) was used to observe the outer surface morphology of the membranes obtained by different pore-forming agents. The surface areas and the pores distribution were discussed using nitrogen adsorption isotherms. X-ray diffraction analysis was performed on the prepared membranes to determine their degree of crystalline or amorphous nature. The XRD patterns for all the prepared membranes were similar to each other. The membrane prepared by calcium carbonate as a pore-forming agent shows the highest surface area (S_{BET}) of 27.249 m^2g^{-1} and a mean pore diameter of 8.1211 nm with a porous structure.

Keywords Cellulose acetate, membrane, calcium carbonate, sodium carbonate, phase inversion technique, nitrogen adsorption isotherm, SEM, XRD

1. Introduction

Membrane water treatment is a low-cost technology for water resource expansion and contaminated water treatment. Membrane water treatment has superior performance in the removal of particles, microorganisms, and turbidity in natural and wastewater [1]. Membrane technology has received the most attention due to its simple process, low energy consumption, and compatibility with the environment. Phase inversion is a process of controlled polymer transformation from a liquid phase to solid phase. The phase inversion process occurred based on the reduction of the solubility of the membrane-forming polymer in the solvent [2]. There are four basic techniques used to create phase inversion membranes (Figure 1).

Precipitation from the Vapor Phase where once a solvent-polymer mixture is cast on the film; it is placed in a vapor atmosphere that contains a nonsolvent saturated with the same solvent. Due to the high concentration of solvent in the vapor atmosphere, the solvent from the cast film stays instead of evaporates into the atmosphere. Membrane forms by diffusion of nonsolvent into the cast film. Precipitation by Controlled Evaporation where the evaporation of the solvent due to high volatility occurs, causing the composition to have a higher nonsolvent and polymer content.

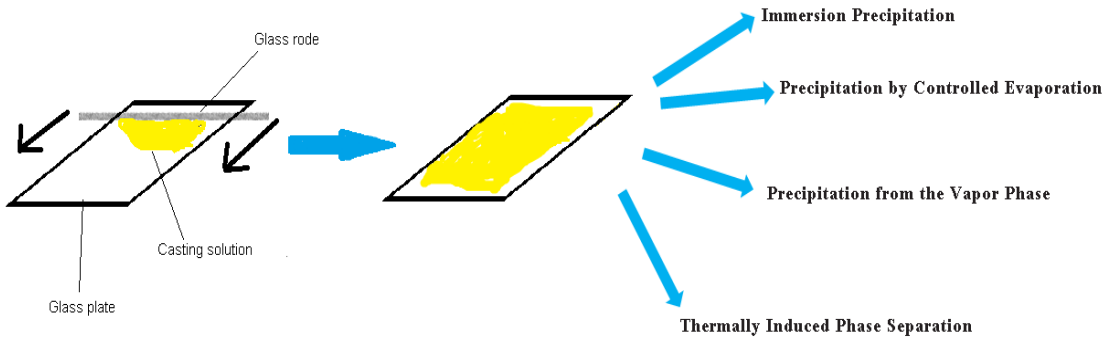

Figure 1: Techniques used to create phase inversion membranes

The polymer eventually precipitates and forms a skinned membrane. Thermally Induced Phase Separation in which a mixed or single solvent polymer solution is cooled down to achieve phase separation. Solvent evaporation induces membrane formation. This method is often used in preparing microfiltration membranes. Immersion Precipitation phase inversion via immersion precipitation is the most widely-used membrane preparation method. A polymer plus solvent (polymer solution) is cast on a proper supporting layer and then submerged in a coagulation bath containing nonsolvent. Due to the solvent and nonsolvent exchange, precipitation takes place. The polymer must be soluble in solvent mixture. The combination of phase separation and mass transfer affects the membrane structure. Out of the four, immersion precipitation is the most widely-used technique for preparing polymeric membranes. The schematic of the membranes production in our work was presented in Figure (2).

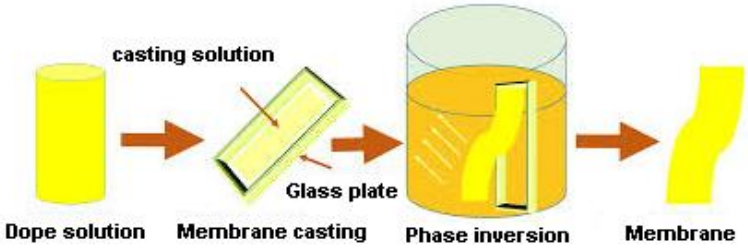

Figure 2: The schematic of the membranes production

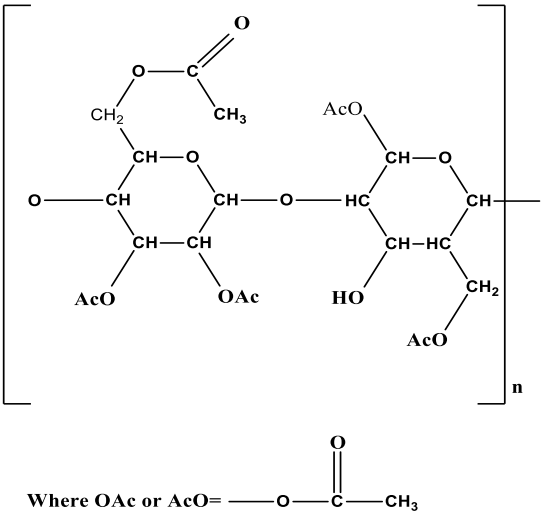

Figure 3: Chemical structure of cellulose acetate polymer

Cellulose acetate Figure (3) is one of the most widely used polymer types for the production of filtration membranes due to its high hydrophobicity, good toughness, high biocompatibility, and resistance to solvents (3). CA is a

semicrystalline insoluble in water but swells due to hydrophilic -OH moieties and acetyl groups on the polymer backbone [4]. Plasticizers are described as low-volatility fluids used to increase the flexibility and extensibility of films by reducing the intermolecular forces between polymer chains to generate the pores such as glycerol, Ni $(NO_3)_2.6H_2O$ and Zn $(NO_3)_2.6H_2O$ [5-7].

2. Experimental

2.1. Materials

Cellulose acetate powder (Mw 50,000; 39.7 wt% acetyl content), acetone (99%), calcium carbonate ($CaCO_3$), sodium carbonate ($NaCO_3$) and hydrochloric acid HCl (37%), all the above-mentioned chemicals were purchased from EL-Naser for chemical and pharmaceutical (Egypt). Distilled water was utilized for solution preparation and glassware cleaning. All chemicals used in this work were of analytical grade, they were used as received, without further purification.

2.2. Preparation of cellulose acetates membranes

To reach to the optimal condition for preparing CA membrane, four membranes were prepared with different contents to make comparison between them. The first one contained 5% CA was prepared by dissolving 1 g of the powder CA in 19ml acetone (5% wt/v) and stirred for 1 h until homogeneous solution formed. The casting solution was static for 1/2 h then poured onto a clean glass plate and dispersed using a glass rod then evaporated in the air for 15 s, finally dried and stored for another use. The second one 1 g of the powder CA was dissolved in 19ml acetone (5% wt/v) and stirred for 1 h. The pore-forming reagent calcium carbonate $CaCO_3$ (1.5gm) was added to the solution and stirred for 1/2 h. The casting solution was static for 1/2 h. The prepared casting solution was poured onto a clean glass plate and dispersed using a glass rod. The nascent membrane was evaporated in the air for 15 s and immersed in a bath of HCl (0.02M) for 1/2h. Then it was being immersed in a deionized water bath several times to eliminate all the calcium carbonate and residual acid. The third one, 1 g of the powder CA was dissolved in 19ml acetone (5% wt/v) and stirred for 1 h. The pore-forming reagent sodium carbonate $NaCO_3$ (1.5gm) was added to the solution and stirred for 1/2 h. The casting solution was static for 1/2 h. The prepared casting solution was poured onto a clean glass plate and dispersed using a glass rod. The nascent membrane was evaporated in the air for 15 s and immersed in a bath of HCl (0.02M) for 1/2h. Then it was being immersed in a deionized water bath. The fourth one containing 10% CA, 2 g of the powder CA was dissolved in 18ml acetone (5% wt/v) and stirred for 1 h. The pore-forming reagent sodium carbonate $NaCO_3$ (1.5gm) was added to the solution and stirred for 1/2 h. The casting solution was static for 1/2 h then poured onto a clean glass plate and dispersed using a glass rod. Finally, it evaporated in the air for 15 s and immersed in a bath of HCl (0.02M) for 1/2h then it was being immersed in a deionized water bath.

2.3. Characterization

The membranes thicknesses (μm) were obtained with the aid of a digital micrometer and the measurements were taken at ten points for each membrane. The textural properties of prepared membranes were determined by physical adsorption – desorption of nitrogen gas at -196ºC using BEL MASTER High pressure adsorption analyzer (BELSORP-HP, Japan) at National Institute of Oceanography and Fisheries. Before each adsorption measurement, the samples were degassed under vacuum at -150ºC and 10^{-5} Torr overnight to ensure adry clean surface. The specific surface area (S_{BET}, m^2/g) was determined by applying the adsorption isotherm using the Brunauer-Emmett-Teller (BET) equation. The adsorption isotherm was constructed as the volume adsorbed (V cm^3/g) versus the equilibrium relative pressure P/P^o, where P is the equilibrium pressure and P^o is the saturation pressure. Determination of S_{BET} by the first part of isotherm ($0.05 < P/P^o < 0.3$) using 0.162 nm^2 as the cross-sectional area of the adsorbed nitrogen molecules. The total pore volume was calculated from the amount of nitrogen adsorbed at a relative pressure (P/P^o) approximately 0.98. The pore size distribution was calculated using the Barrett – Joyner-Halenda (BJH) model. The surface morphology and topographic analysis of the prepared membranes were examined by Scanning Electron Microscope (SEM) JSM-5300 (JEOL Ltd., Japan) instrument with a 30 kv accelerating voltage. Prior to the measurement, the samples were dried at 110 ºC for 4 h. The samples were coated with a thin

layer of gold for charge dissipation to clear visibility of the surface morphology [8]. Fourier transform infrared spectra (FTIR) were recorded in the range between, 4000 and 400 cm^{-1} on a Perkin Elmar FT-IR (FRONTIER OPTICA + SP10 STD, L1280032, USA) at National institute of Oceanography and Fisheries in Alex. X – ray diffraction analysis was performed on the prepared samples to determine the degree of crystalline or amorphous nature of the prepared membrane. Powder diffractometry (XRD) was detected via (Shimadzu 7000) diffractometer with Cu-Kα radiation beam (λ= 1.5406 A^o).

3. Results and Discussion

Four membranes were prepared (M_1, M_2, M_3 and M_4) with different contents to reach to the optimal condition for preparing CA membrane Table (1).

Table 1: The contents of the prepared membranes

Membrane	Solvent	CA(%)	$CaCO_3$(g/100ml)	Na_2CO_3
M_1	acetone	5%	_____	_____
M_2	acetone	5%	7.5	_____
M_3	acetone	5%	_____	7.5
M_4	acetone	10%	_____	7.5

3.1. Thickness

It was noted that the addition of glycerol contributed to increasing the thickness of the cellulose acetate membranes [9,10]. The prepared membrane thicknesses are displayed in Table (2). In this approach, the plasticizer's presence may have triggered a certain disarray and breakdown of the intra- and intermolecular connections of the polymeric material, which led the chains to disperse and resulted in an increase in membrane thickness.

Table 2: Average values of the thickness of the cellulose acetate membranes

Membrane	Thickness (µm)
M_1	40.34
M_2	43.16
M_3	43.32
M_4	44.67

3.2. N_2 adsorption isotherm

Figure (4) shows nitrogen adsorption-desorption isotherms of M_1, M2, M3 and M4 membranes. The four samples exhibited adsorption isotherm of type IV, showing a hysteresis loop at relative pressures above 0.3. The similar shapes, i.e. with a steep curve at the low-pressure range, then parallel to the relative pressure axis at the high-pressure range. The adsorption and desorption branches followed nearly the same path with a relatively narrow hysteresis loop. The observation of a hysteresis loop indicates the presence of wider pores, which may be related to the effect of Na_2CO_3, $CaCO_3$ and glycerol. This type of hysteresis loop is attributed to cylindrical pores and or the 'ink bottle' pores [11]. According to the IUPAC recommendation hysteresis classified into types H1, H2, H3 and H4 as shown in Figure (4). All the studied membranes gave isotherm with type H4 in which parallel and almost horizontal branches and this is often associated with narrow slit pores. The values of surface area S_{BET} (m^2/g), total pore volume V_T(mL/g) and pore radius(nm) are summerized in Table (3). The BET constant is considering a measure of the heat of adsorption or in other words the strength of the interaction in the first adsorbed layer. the surface area of M_1 membrane (18.919 m^2/g) and total pore volume (0.02434 mL/g) are low due to the absence of pore forming agents. In case of M_2 membrane on using $CaCO_3$ as pore forming agent the surface area was increased to 27.249m^2/g with 44.03 % increases in relative to M_1 membrane and total pore volume of 0.038411mL/g. For M_3

membrane on using Na_2CO_3 and glycerol the surface area was (21.745m^2/g) and total pore volume also was (0.02779mL/g) with 14.94 % increases in relative to M_1 membrane. This fact is due to its ability to form more pores, which increase the surface area of the membrane due to the interruption of the polymeric structure of cellulose acetate on adding Na_2CO_3 as pore forming agent. M_4 membrane was showing the lowest surface area of 10.698m^2/g with total pore volume of 0.016878mL/g due to increasing the cellulose acetate percentage from 5 to 10 % which difficult the role of the pore forming agent. The mean pore diameter of M_1(3.5734nm) and M_2 (8.1211nm) consists basically of mesopores, which are defined by IUPAC as pores has a radius from 2 to 50 nm. In case of M_3 and M_4 it was found that there pores radius were 5.1120 and 6.3109nm respectively, which related to the mesopores formed according to the IUPAC classification. The results show that the pore forming agents were efficient in terms of generating pores and increasing the specific surface area of the membranes.

Table 3: The comparison between the prepared membranes M_1, M_2, M_3 and M_4

Membrane	Mean pore diameter (nm)	S_{BET} (m^2g^{-1})	Total pore volume(cm^3g^{-1})
M_1	3.5734	18.919	0.02434
M_2	8.1211	27.249	0.038411
M_3	5.1120	21.745	0.027790
M_4	6.3109	10.698	0.016878

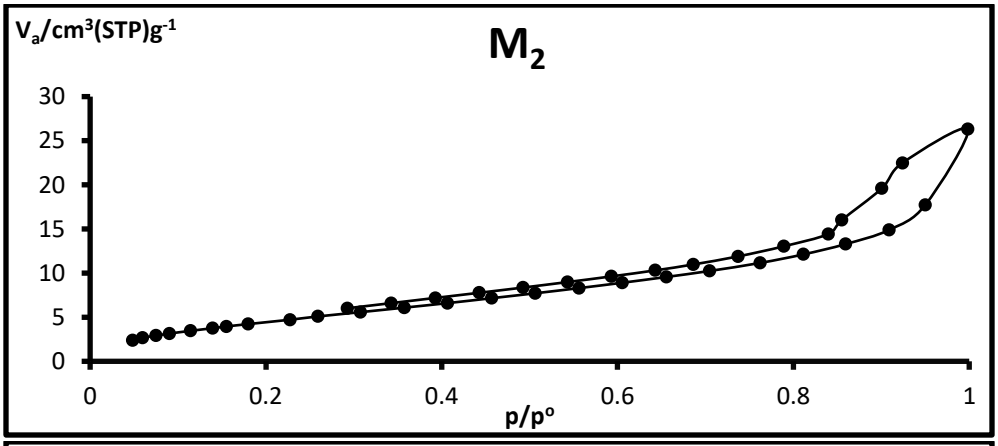

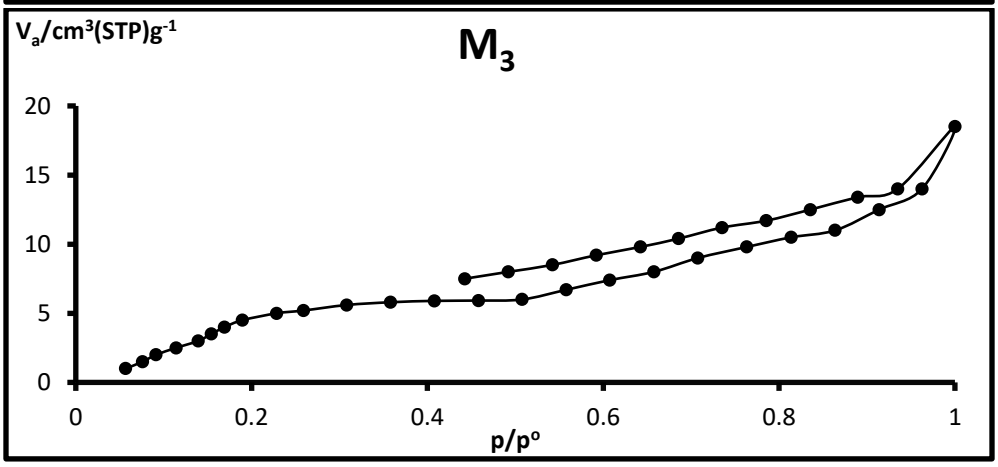

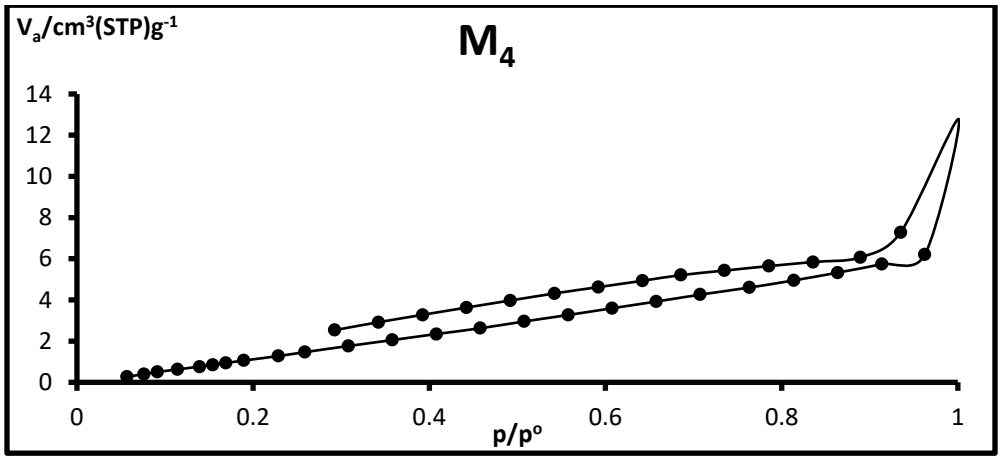

Figure 4: The Nitrogen adsorption /desorption isotherms for of the prepared membranes M_1, M_2, M_3 and M_4.

3.3. Scanning electron microscopy analysis (SEM)

Figure (5a and 5b) shows a smooth and homogeneous membrane surface for M_1 where the cellulose acetate was used without any pore forming agent. In case of M_2, M_3 and M_4 membranes already show surface containing pores of different diameters and depth. This is related to the effect of the pore forming agents (Na_2CO_3 and $CaCO_3$) that they disrupt the cellulose acetate chains and breaking the microfibrillar structure. It is highly observed that M_2 membrane has smaller pores with homogeneous distribution on the membrane surface Figure (5c and 5d). M_3 and M_4 membranes have bigger pores with heterogeneous distribution on the membranes surfaces Figure (5e,f and 5g,h). M_4 membrane showing smaller pores than M_3 due to the increase in the cellulose acetate percentage in case of M_4 membrane which decrease the effect of Na_2CO_3 on generating large pores. Hence, the presence of the pore forming agents (Na_2CO_3 and $CaCO_3$) and glycerol modified the polymer network and causing internal morphological changes which reflected with the appearance of pores with different size [12].

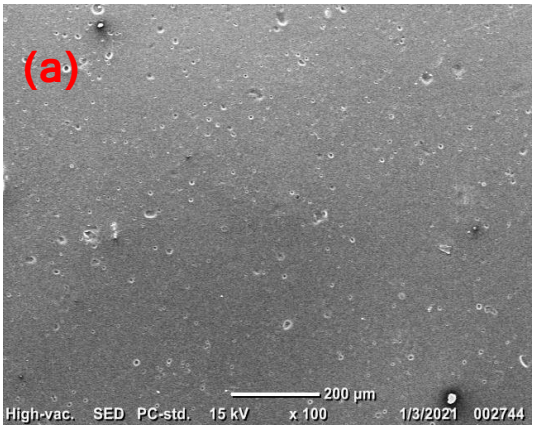

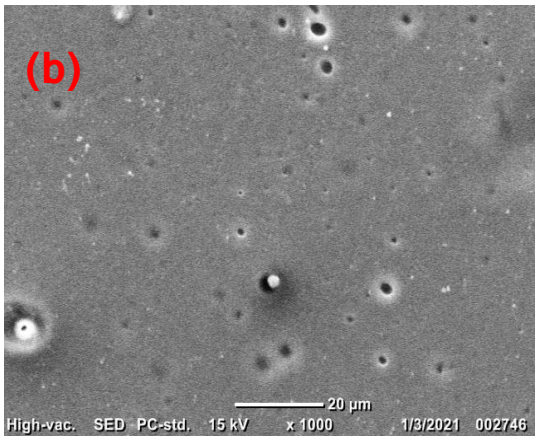

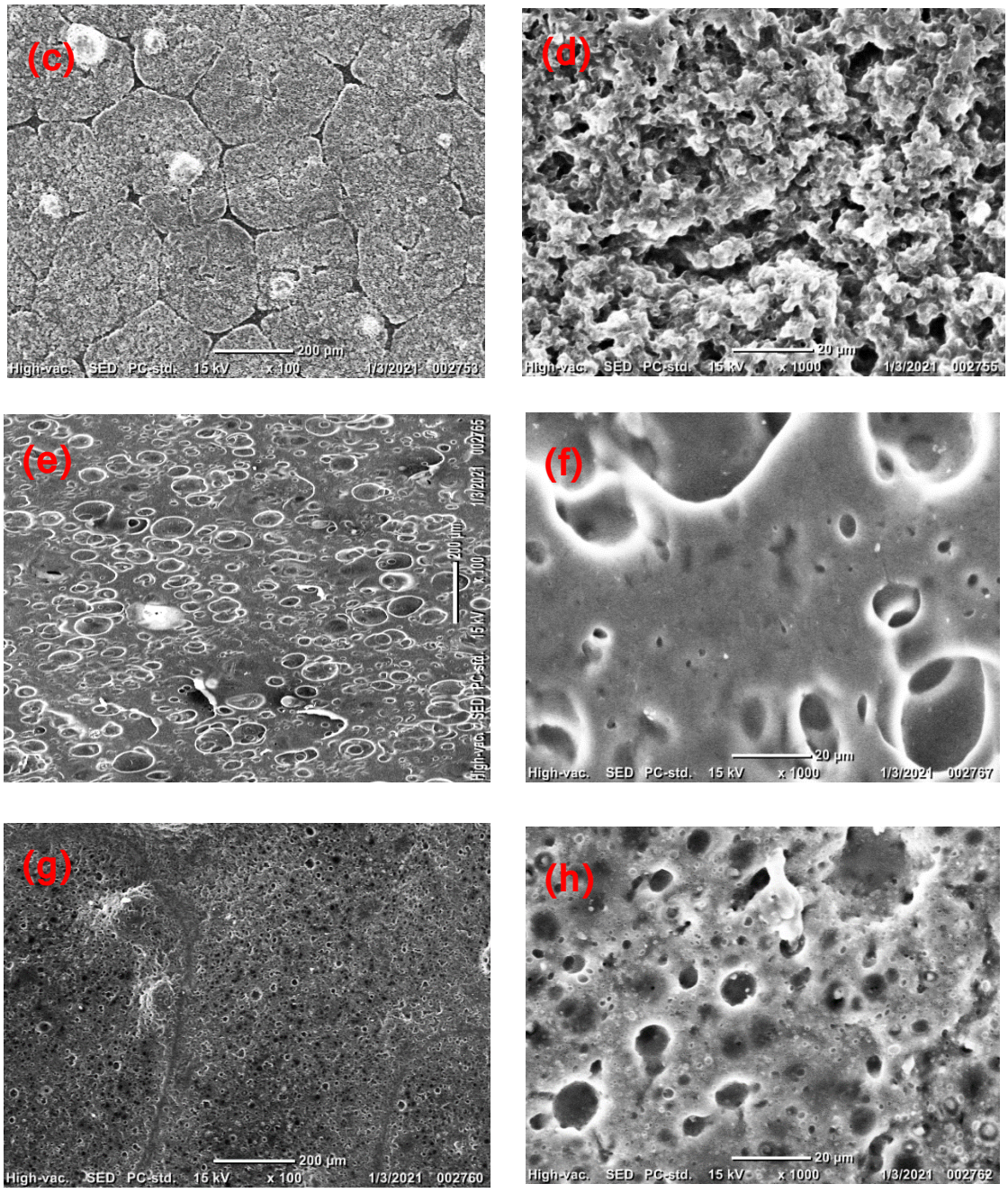

Figure 5: The SEM micrographs of the prepared membranes (M_1 (a and b)); M_2 (c and d); M_3 (e and f) and M_4 (g and h)) at different magnification

3.4. FTIR spectroscopy

The surface functional group of the CA membrane (M_2) was evaluated by FTIR Figure (6). For CA membrane (M_2), the obtained spectra showed peak at 3480cm^{-1} representing –OH stretching [13]. The band at 2935 cm^{-1} represents the aliphatic of C-H group. The band at 1750 cm^{-1} is attributed to the stretching vibration of C=O bond, the band at 1616 cm^{-1} related to c=c aromatic and a band at 1400 cm^{-1} shows O-H group. The characteristic bands around 1475 cm^{-1} represent the bending vibration of CH_2. The bands at 1373 and 1230 cm^{-1}, corresponding to the characteristic band of C–O and C–H of acetyl group (CHCOO), respectively. 1226 cm^{-1} assigned stretching vibration of the C-O

group and the band at 900 cm^{-1} corresponding to the out-of-plane C-H bend [14]. Moreover, the bands located in 1038 cm^{-1} is caused by hydroxyl ring of cellulose ether. The peaks around 1050cm^{-1} correspond to the stretching of the C-O bond. These features were signature peaks of lignocellulosic material [15].

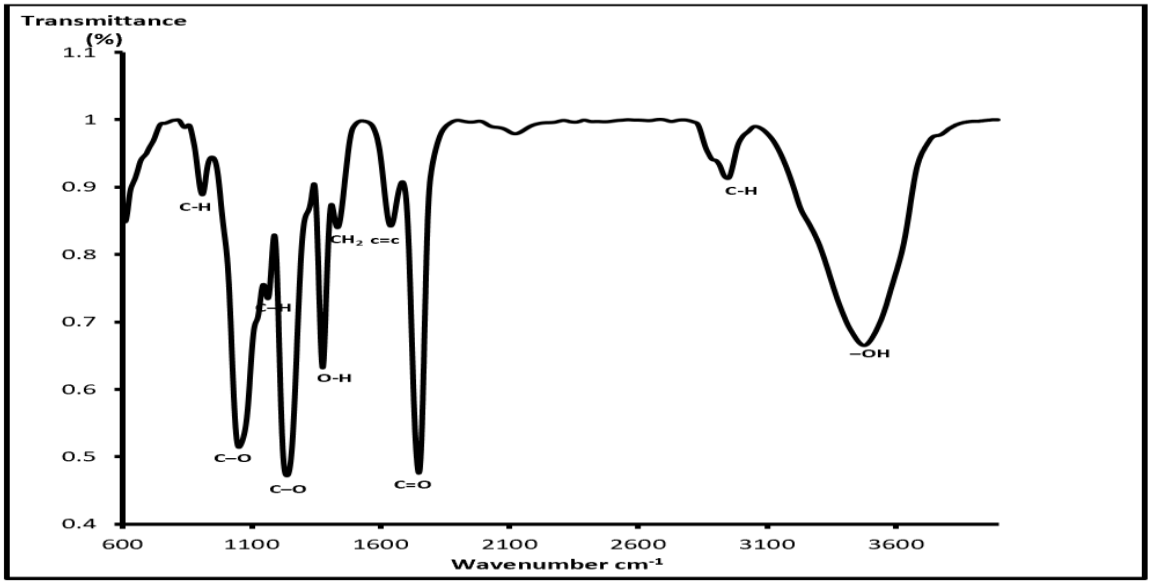

Figure 6: FTIR – spectra of cellulose acetate membrane (M_2)

3.5. X–ray diffraction (XRD)

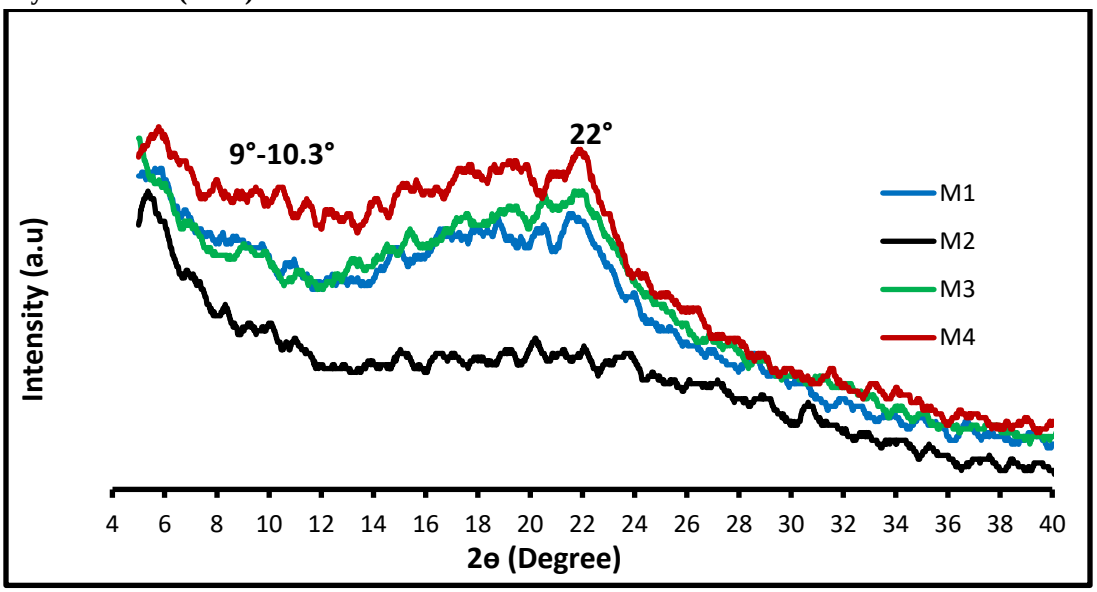

Figure 7: The XRD for of the prepared membranes M_1, M_2, M_3 and M_4

4. Conclusions

The present work provides a simple and easy production process for the fabrication of polymeric membranes. The uses of pore forming agents were effective on creation of pores with the possibility to adapt pore size and morphology. The use of $CaCO_3$ as pore forming agent was preferred that it providing a high surface area of

27.249m^2/g with 44.03 % increases in relative to cellulose acetate only without pore forming agents and total pore volume of 0.038411mL/g.

Acknowledgments

I would like to gratefully acknowledge the help, support and inspiration I received, and express my deep gratitude to my supervisors for their valuable guidance, thoughtful criticism, informative and continuous observation throughout the work.

Competing interests

The authors declare that they have no known competing financial interests or personal relationships that could have appeared to influence the work reported in this paper.

Funding

No funding was received.

Availability of data and materials

I understand that my manuscript and associated personal data will be shared with Research Square for the delivery of the author dashboard. The data will be available upon request.

Authors' contributions

Author contribution All authors contributed to the study conception and design. Material preparation, data collection, and analysis were performed by Rehab E. Elwardany, Hassan Shokry, Ahmed A. Mustafa, Alaa E. Ali.

References

[1]. Xie, J., & Hung, Y. C. (2019). Methodology to evaluate the antimicrobial effectiveness of UV-activated TiO2 nanoparticle-embedded cellulose acetate film. Food Control, 106, 106690.

[2]. Lee, H.J., Jung, B., Kang, Y.S., Lee, H., 2004. Phase separation of polymer casting solution by nonsolvent vapor. J. Membr. Sci. 245, 103e112.

[3]. Abedini, R., Mousavi, S. M. & Aminzadeh, R. (2011). A novel cellulose acetate (CA) membrane using TiO2 nanoparticles: Preparation, characterization and permeation study. Desalination, 277, 40-45.

[4]. Perera, D. H. N., Nataraj, S. K., Thomson, N. M., Sepe, A., Hüttner, S., Steiner, U., . . . Sivaniah, E. (2014). Room-temperature development of thin film composite reverse osmosis membranes from cellulose acetate with antibacterial properties. Journal of Membrane Science, 453, 212-220.

[5]. M. Akbarzadeh, M.T. Vardini, G.R. Mahdavinia, Preparation of a novel magnetic nanocomposite hydrogel based on carboxymethyl chitosan for the adsorption of crystal violet as cationic dye, J. Chem. Health Risks. 8 (4) (2018) 289–304.

[6]. S. Mani, R.N. Bharagava, Exposure to crystal violet, its toxic, genotoxic and carcinogenic effects on environment and its degradation and detoxification for environmental safety, Rev. Environ. Contam. Toxicol. 237 (2016), https://doi.org/ 10.1007/978-3-319-23573-8_4.

[7]. Lee, W. G., & Kang, S. W. (2020). Eco-friendly process for facile pore control in thermally stable cellulose acetate utilizing zinc (II) nitrate for water-treatment. Journal of Industrial and Engineering Chemistry, 81, 88-92.

[8]. Hassan A. F., and Elhadidy H., (2017). Production of activated carbons from waste carpets and its application in methylene blue adsorption: Kinetic and thermodynamic studies, journal of environmental chemical engineering. 01: 003.

[9]. Farias, M. G., Fakhouri, F. M., Carvalho, C. W. P. D., & Ascheri, J. L. R. (2012). Caracterização físico-química de filmes comestíveis de amido adicionado de acerola (Malphigia emarginata DC). Química Nova, 35, 546-552.

[10]. Aimoto Shimazu, A., Mali, S., & Victória Eiras Grossmann, M. (2007). Plasticizing and antiplasticizing effects of glycerol and sorbitol on biodegradable cassava starch films. Semina Ci. agr., 79-88.

[11]. Frost R. and Carmody O. and Xi Y. and Kokot S., (2007), Surface characterization of selected sorbent materials for common hydrocarbon fuels. Surface Science, 601(9): 2066-2076.

[12]. Gonçalves, S. M., Dos Santos, D. C., Motta, J. F. G., Dos Santos, R. R., Chávez, D. W. H., & de Melo, N. R. (2019). Structure and functional properties of cellulose acetate films incorporated with glycerol. Carbohydrate polymers, 209, 190-197.

[13]. Pontes, S. F. O. (2013). Desenvolvimento de nanoemulsões de óleos essenciais incorporadas em filme de metilcelulose para uso em alimentos.

[14]. Zafar, A., Bertocco, F., Schjødt-Thomsen, J., & Rauhe, J. C. (2012). Investigation of the long term effects of moisture on carbon fibre and epoxy matrix composites. Composites Science and Technology, 72(6), 656-666.

[15]. K.O. Reddy, C.U. Maheswari, M. Shukla, J.I. Song, A.V. Rajulu, Tensile and structural characterization of alkali treated Borassus fruit fine fibers, Compos. Part B 44 (2013) 433–438, https://doi.org/10.1016/j.compositesb.2012.04.075.

[16]. Daud, W. R. W., & Djuned, F. M. (2015). Cellulose acetate from oil palm empty fruit bunch via a one step heterogeneous acetylation. Carbohydrate Polymers, 132, 252-260.

[17]. Zheng, W., Chen, L. J., Yang, G., Sun, B., Wang, X., Jiang, B., Yin, G.Q., Zhang, L., Li, X., Liu, M. & Yang, H. B. (2016). Construction of smart supramolecular polymeric hydrogels cross-linked by discrete organoplatinum (II) metallacycles via post-assembly polymerization. Journal of the American Chemical Society, 138(14), 4927-4937.